©2017 RSSJ Journal of The Remote Sensing Society of Japan Vol. 37 No. 3 (2017) pp. 248-260

Original Paper

Urban Growth Modeling based on the Multi-centers of the Urban Areas and Land Cover Change in Yangon, Myanmar

Tanakorn SRITARAPIPAT* and Wataru TAKEUCHI*

Abstract

Yangon, the former capital of Myanmar, is the major economic areas of the country. Also, the urban areas have significantly increased. However, Yangon has problems with disasters such as flood and earthquake. To support disaster risk management in Yangon, Myanmar, the estimation of urban expansion is required to understand the mechanism of urban expansion and predict urban areas in the future. This research proposed a methodology to develop urban expansion modeling based the dynamic statistical model using Landsat Time-Series and GeoEye Images. Multispectral Landsat images from 1978 to 2009 were classified to provide land cover change with a long period. By observing land cover from the past to the present, the class translation matrix was obtained. Stereo GeoEye Images in 2013 were employed to extract the heights of buildings. By using the heights of buildings, the multi-centers of urban areas cloud be detected. The urban expansion modeling based on the dynamic statistical model was defined to refer to three factors; (1) the distances from the multi-centers of the urban areas, (2) the distances from the roads, and (3) the class translation. The estimation of urban expansion was formulated in term of the dynamic statistical model by using the maximum likelihood estimator. The relevant equations to estimate urban expansion are expressed in this research. The prediction of urban expansion was defined by the combination of the estimation of urban expansion and the estimated parameters in the future. In the experiments, the results indicated that our model of urban expansion estimated urban growth in both estimation and prediction steps with efficiency.

Keywords : Urban expansion; Dynamic statistical model; Landsat; GeoEye

1. Introduction

Yangon, formerly known as Rangoon, is the largest city in Myanmar, formerly known as Burma. Yangon is the major of country's economic areas with more than five million population, and the urban areas have significantly increased[1]. However, Yangon has suffered from the series of floods and it had faced the effect of the earthquake in 1930. To support disaster risk management in Yangon, Myanmar, we need to understand the phenomena of urban expansion and create the model of urban expansion to predict urban areas in the future.

Urban growth is rather a complex process. Since urban expansion causes from many factors such as human behaviors, population rates, the economic states, the policies of the government and so on. Remote sensing technology provides the physical information that can directly monitor the urban areas from the past to the present. Hence, it can lead us to understand the mechanism of urban expanding or how urban expands[2]. In the other hand, by understanding the system of urban expansion, the urban expansion modeling can be created to predict urban areas in the future[3]. This information can be used to support urban development and management for urban planning or decision-making.

The various kinds of urban expansion models have been widely developed in order to understand the system of urban expansion and predict the urban areas in the future. Urban land-use model based on spatial interaction model was developed[4]. Spatial interaction model known as the gravity model was described the spatial relations between two objects. All interactions in the system are the spatial relations between any pairs of all objects. By using the interactions, the estimated urban areas can be generated. Next, the statistical model was used for introducing urban expansion model. The model relies on a mathematical mechanism. For the example work from Sklar[5], the statistical model was defined as a set of equations relating the population growth and the land-use change. Next, an urban growth model based on automata cellular was proposed[6]. The automata cellular model refers to cell space with the pixel and neighboring pixels including the transition rules from land use change. Moreover, by using multi-agent-based model, the residential distribution estimation was developed[7]. The Multi-agent system model; including the automata cellular model with translation rules and relating to human behaviors and the

(Received November 2, 2016. Accepted May 29, 2017)
* Institute of Industrial Science, The University of Tokyo, 4-6-1 Komaba, Meguro-ku, Tokyo, 153-8505, Japan

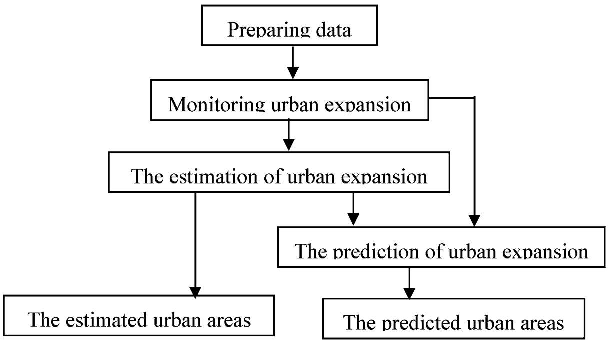

Fig. 1 Flowchart of our methodology.

environments, cloud be used to simulate urban areas in efficacy.

In the common model of urban expansion such as the automata cellular model, the observed statistical data such as mean and variance have been not included in the model, the model will estimate the urban expansion without taking the advantage of the statistical data. Whereas, this research aims to use the dynamic statistical data to support the model of urban expansion to estimate the urban expansion with reliability and accuracy. Another point is to estimate urban expansion with the distances from the multi-centers of urban areas that can be assumed as the facility communities and are able to be detected by Remote Sensing technology.

This research introduced a methodology to develop urban expansion modeling based on the dynamic statistical model by using the multi-centers of the urban areas and land cover change in Yangon, Myanmar. We used Landsat 1−7 images from 1978 to 2009 and Stereo GeoEye images as well as the locations of the roads. The details of our methodology are described in section 2. The experimental results with the discussions are given in section 3. Finally, the conclusions of this research are presented in section 4.

2. Methodology

2. 1 Modeling urban expansion

Generally, urban expansion is considered on three aspects with (1) facility, (2) transportation, (3) environment[8)9)]. In this research, we defined that urban expansion in Yangon, Myanmar is related to (1) the distances from the multi-centers of urban areas for facility aspect, (2) the distances from the roads for transportation aspect, (3) the class translation for environment aspect. For the first factor of the distances from multi-centers of urban areas, we defined that the multi-centers of urban areas are the groups of the high-rise buildings such as department store, hotel, office, and school. We supposed that in the city, there are many centers of the urban areas. The new urban areas should be located near the multi-centers of urban areas that can be assumed as the facility communities. For the second factor of the distances from the roads, the people set up the houses near the roads since it is convenient for transportation. For the third factor of the class translation, the urban grow up from the vegetation areas more than from water areas. In this research, we assumed that urban expansion is non-urban areas that changed to urban areas. The flowchart of our methodology to model urban expansion is displayed in figure 1.

Table 1 The details of remotely sensed dataset in this research.

No.	Satellite and Sensor	Bands	Resolution	Acquired Date
1	Landsat -3 MMS	4	60m. x 60m.	1978-11-22
2	Landsat -4 TM	7	30m. x 30m.	1990-11-12
3	Landsat -7 ETM	8	30m. x 30m.	2000-11-7
4	Landsat -5 TM	7	30m. x 30m.	2009-11-08
5	GeoEye RGB (Stereo)	3	0.5m x 0.5m.	2013-11-08 2013-11-16

2. 2 Preparing data for urban expansion model

The study location of this research was focused on Yangon, Myanmar from 16.73106° to 17.00594° North and 96.02452° to 96.31000° East. In this research, four multispectral Landsat images with a 30-m. resolution and 1,000×1,000 pixels from 1978 to 2009 (almost every ten years) were used to provide the land cover change. Stereo GeoEye images with a 0.5 m.-resolution were employed to extract the heights of buildings. The Geographic Information Systems (GIS) data of the roads were provided in the format of polyline in 2013 by International Center for Urban Safety Engineering (ICUS), The University of Tokyo, Japan. The details of the remotely sensed dataset are shown in table 1 and the images from Landsat and GeoEye are displayed in figure 2. Since the Landsat image in 1978 has the original resolution of 60 m., it was converted to be the resolution of 30 m. by the nearest-neighbor interpolation. The GIS data of roads was transformed into the resolution of 30 m. The estimated heights of the buildings were converted into the resolution of 30 m.

For obtaining the land cover change from 1978 to 2009, the Landsat images were classified into three classes of (1) urban, (2) vegetation, and (3) water by using Mahalanobis distance method[10)] (supervised classification). We selected the examples with more than 500 samples in each class. After computing the classification, there are still some noises in the classification results causing from cloud effects for the Landsat image in 1990 and the low resolution for the Landsat image in 1978 (mixed classes in one pixel). To improve the classification results, the rules of urban expansion and removing cloud effect were applied. For the rule of urban expansion, we assumed that the

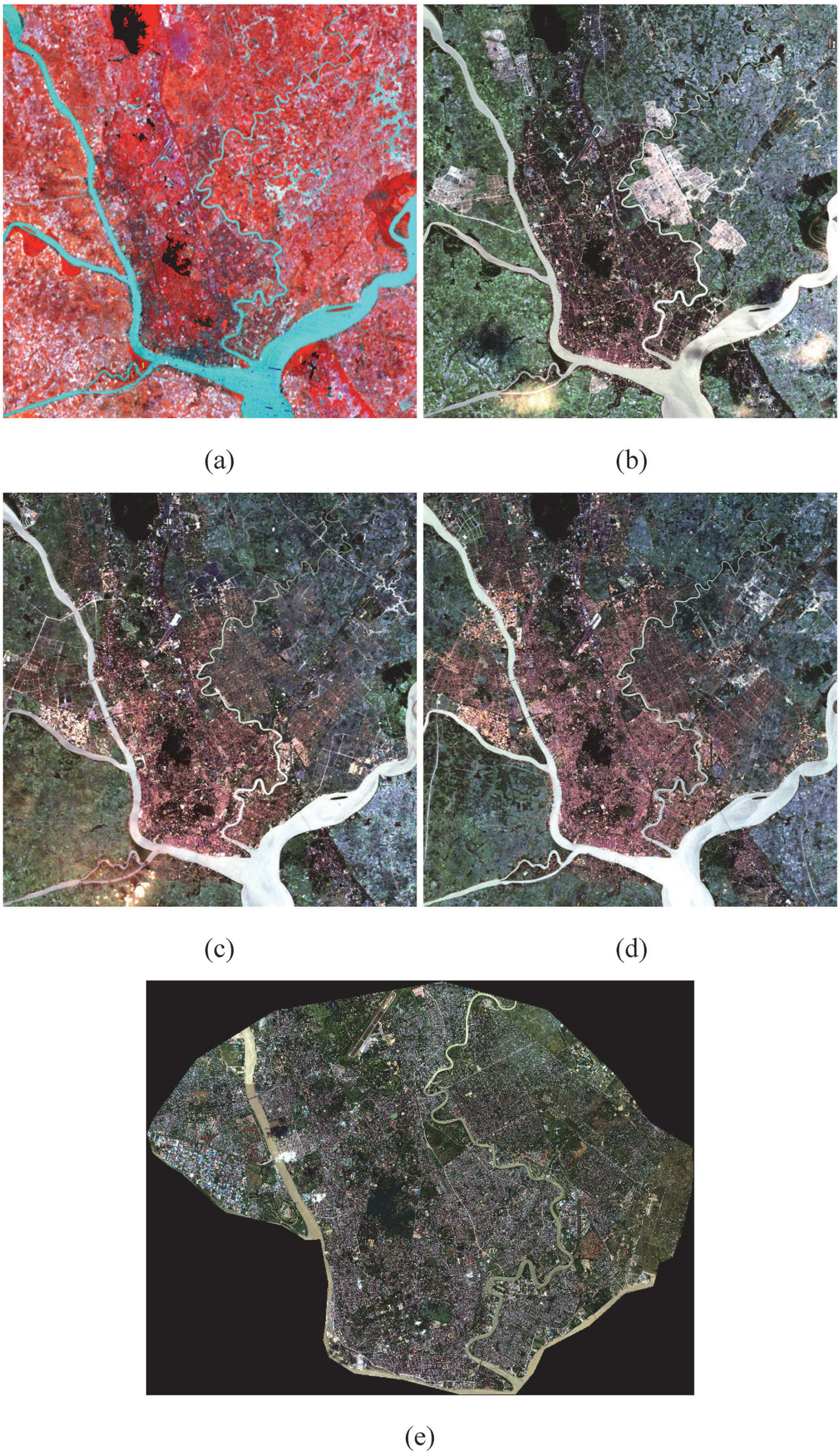

Fig. 2 (a) the Landsat image in 1978 (False color), (b) the Landsat image in 1990, (c) the Landsat image in 2000, (d) the Landsat image in 2009, (e) the GeoEye image in 2013.

urban areas always expand and then we defined that vegetation and water can change to urban, but urban cannot change to vegetation and water. For the rule of removing cloud effects that made the incorrect result, we defined that the pixels affected by clouded areas in the classification result in 1990 by manually search are replaced by the pixels in the classification result in 1978 (the previous time result without clouded areas). The improved classification results in 1978, 1990, 2000 and 2009 are shown in figure 3 and 11 (a, c, e), respectively. For validation, we compared the land cover result in 2009 with a land cover map in 2012 provided by ICUS. The accuracy of the land cover result in 2009 is 78% with Kappa coefficient of 0.71. The statistics of land cover change over Yangon from 1978 to 2009 is depicted in figure 4.

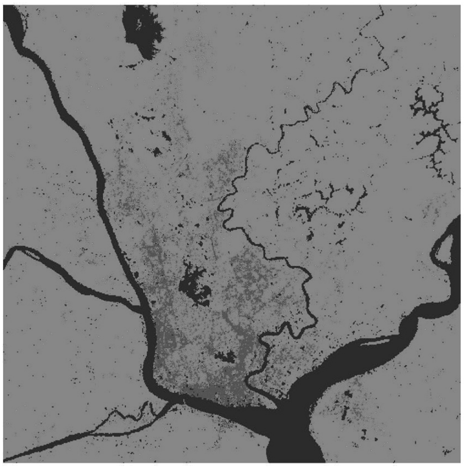

Fig. 3 The land cover result in 1978

For detecting the multi-centers of urban areas, the stereo GeoEye images were extracted to obtain Digital Surface Model (DSM). The DSM was filtered by the Morphological filter to get Digital Terrian Model (DTM). By subtracting DSM with DTM, the height of the building was provided (figure 5 (a)). Then, the heights of the buildings were separated into two classes of (1) low and (2) high buildings by manual thresholding with the threshold value of 10 meters. After that, the locations of the high buildings were grouped into seven classes by using K-means (Unsupervised classification). By consideration of urban expansion data and the heights of the buildings by human perspective, in Yangon, we observed that there are seven locations that significantly effect to urban expansion. Hence, we set the number of classes for K-means method as seven classes. The center positions of seven classes were defined as the locations of the multi-centers of the urban areas (figure 5 (b)). The regions of the multi-center areas with the Voronoi tessellation are displayed in figure 5 (c).

2. 3 Monitoring urban expansion

We monitored urban expansion data extracted from the classification results from 1978 to 2009 by relating to the defined factors with (1) the distance from the multi-centers of the urban areas, (2) the distance from the roads, (3) the class translation. In this research, urban expansion refers to non-urban areas that changed to urban areas.

For monitoring urban expansion relating to the distance from the multi-centers of the urban areas, we calculated the Euclidean distances of non-urban pixels that changed to urban from the pixels to the nearest center of the urban areas in each region. The means and variances of the Euclidean distance from the multi-

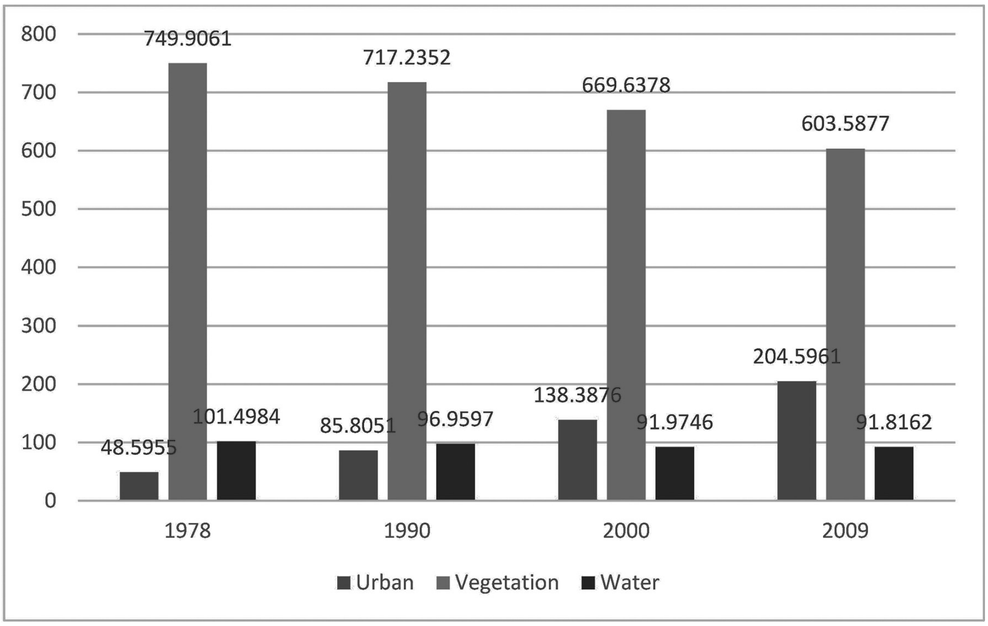

Fig. 4 The statistics of land cover change over Yangon City (The unit of sq.km.).

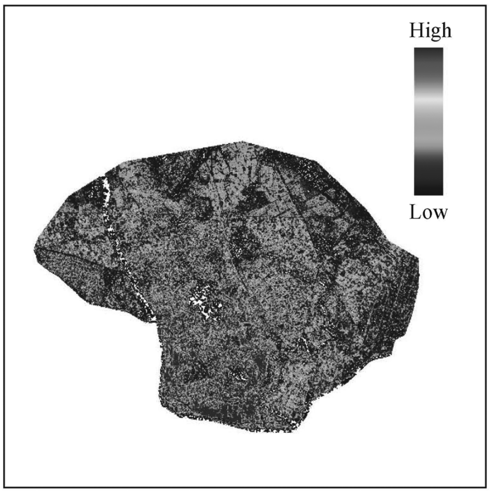

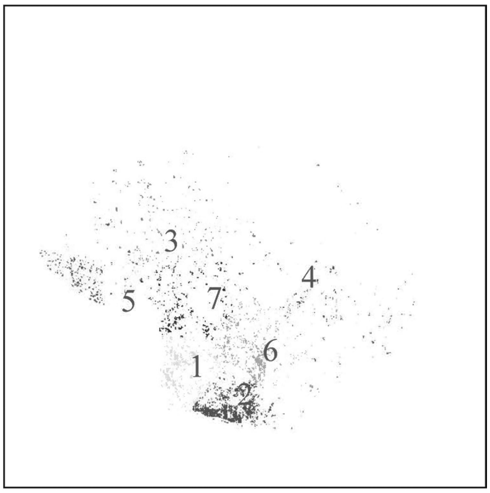

(a) (b)

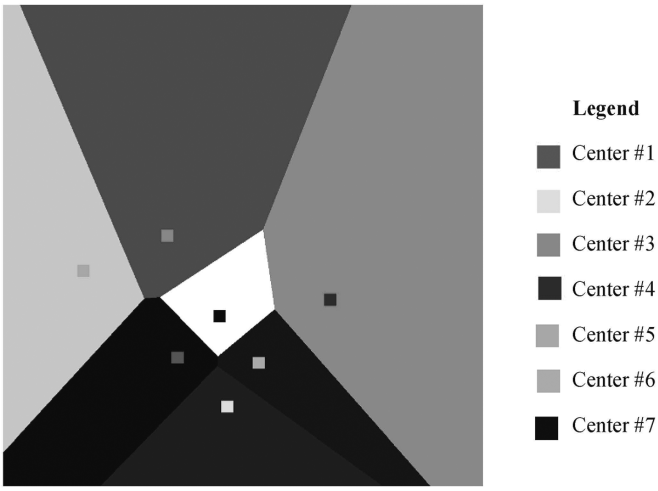

(c)

Fig. 5 (a) the heights of the buildings (b) the classification result of the multi-centers of urban areas, and (c) the Voronoi tessellation with seven locations of the multi-centers of urban areas.

Table 2 The means and variances of the Euclidean distance from the multi-centers of urban areas in each region from 1978 to 2009 (The unit of pixel).

Region	1978→1990		1990→2000		2000→2009	
	Mean	Variance	Mean	Variance	Mean	Variance
Center #1	87.1	4,411	90.2	4,260	87.5	4,608
Center #2	81.5	2,394	96.7	1,975	89.9	1,778
Center #3	171.3	11,376	199.3	14,568	239.4	14,444
Center #4	140.8	6,607	133.7	8,602	195.4	14,686
Center #5	116.7	2,452	76.9	3,900	139.7	6,702
Center #6	98.8	4,267	118.2	7,801	151.2	13,577
Center #7	127.0	3,011	141.9	3,428	129.8	3,425

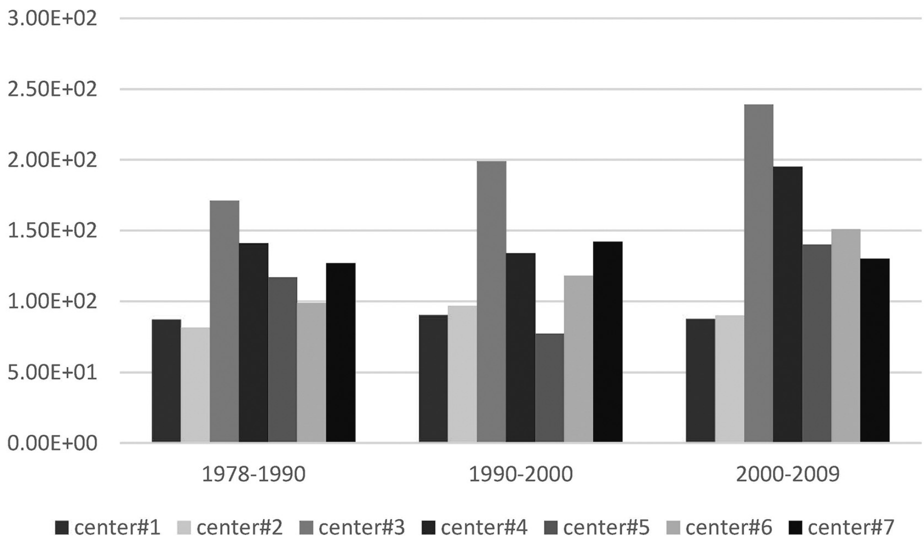

Fig. 6 The bar graphs of the means of the Euclidean distance from the multi-centers of urban areas in each region from 1978 to 2009 (The unit of a pixel).

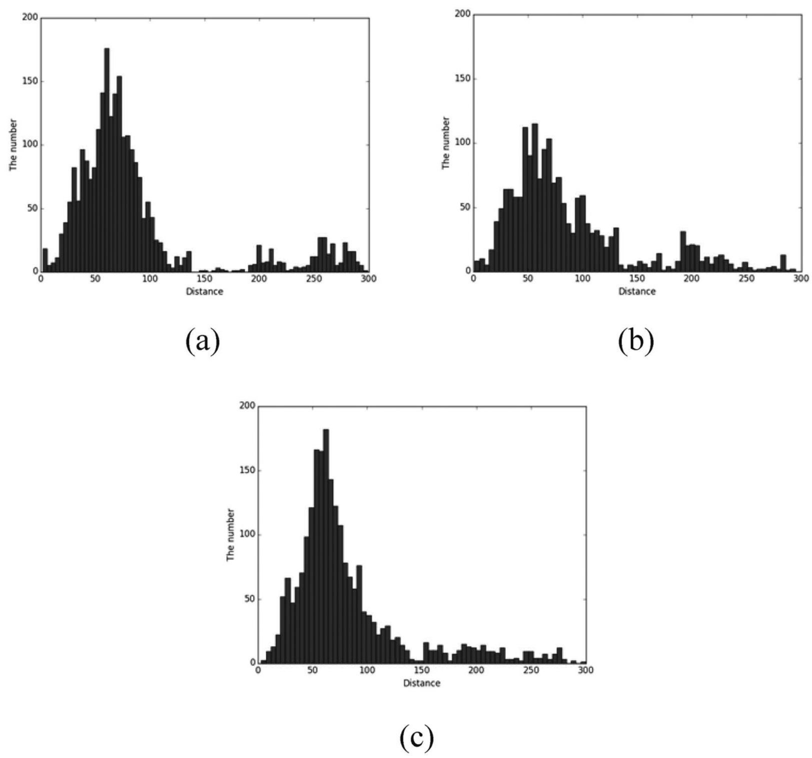

Fig. 7 The histograms of the Euclidean distance from the multi-centers of urban areas in the region of the center #1 in the years of (a) 1978 → 1990, (b) 1990 → 2000, (c) 2000 → 2009 (The unit of a pixel).

centers of the urban areas in each region from 1978 to 2009 are shown in table 2, and figure 6 displayed the means of the Euclidean distances from the multi-centers of urban areas in term of bar graphs. The examples of the histograms of the Euclidean distances from the multi-centers of the urban areas in the region of the center #1 with time variation are depicted in figure 7.

According to the increasing values of the means of the Euclidean distance from the multi-centers of urban areas from 1978 to 2009 in the almost regions (see in figure 6), we investigated that the urban expanded from the near distance from the multi-centers of the urban area to the far distance. The distributions of the histograms seem as the Gaussian distributions (see in figure 7).

For monitoring urban expansion to the distance from the roads, we calculated the Euclidean distances of non-urban pixels that changed to urban from the pixels to the nearest roads. The

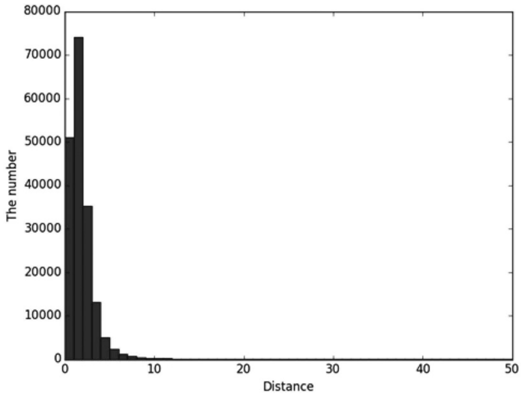

Fig. 8 The histogram of the Euclidean distances from the roads (The unit of a pixel).

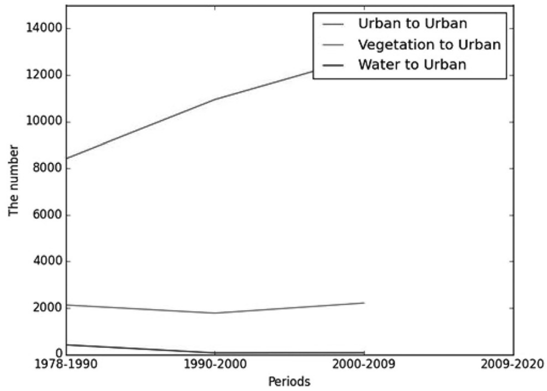

Fig. 9 The class translation in the region of the center #1 from 1978 to 2009 (The unit of pixel).

Table 3 The class translation in the region of the center #1 from 1978 to 2009 (The unit of pixel).

	1978-1990	1990-2000	2000-2009
urban→urban	8,410	10,942	12,780
vegetation→urban	2,123	1,774	2,208
water→urban	409	64	69

mean and variance of the Euclidean distance from the roads are 1.42 and 4.34, respectively. The histogram of the Euclidean distances from the roads is shown in figure 8.

We found that the urban grew up along the roads, and the distribution appears as the Gamma distribution (see in figure 8).

For monitoring urban expansion relating to the class translation, we observed the number of vegetation and water (non-urban) turn into urban from the land cover change from 1978 to 2009. The examples of the class translation in the region of the center #1 with time variation are illustrated in table 3 and figure 9 in term of a line graph.

We found that the urban grew up from vegetation more than from water. In this research, we defined that urban always change to urban. Also, the urban expansion refers to non-urban (vegetation and water) that changed to urban. Therefore, the class translation from urban to urban was not included in our model.

2. 4 The estimation of urban expansion

In this research, the maximum likelihood estimator was used to estimate urban expansion[11]. By using the estimator, we need to maximize the probabilities of the defined factors with (1) the distance from the multi-centers of urban areas, (2) the distance from the roads, (3) the class translation by observing urban expansion. In this research, the Gaussian distribution was used in our model since it is generally used in the common case for physical variables. Also, it is suitable for large size samples since when the samples are very large, they always incline as the Gaussian distribution. Since urban areas generally grow up, the samples will be increased. As a result, the probability of the distance from the multi-centers of the urban areas was assumed as the Gaussian distribution with time variation. Whereas, the probability of the distance from the roads looks like the Gamma distribution than the Gaussian distribution. However, for the simpler model, the probability of the distance from the roads was defined as the Gaussian distribution without time variation. The probability of the class translation with time variation was defined as Markov chain. For class translation, in this research, urban expansion refers to non-urban areas that changed to urban areas. The class translation from non-urban to urban is only used in this model. The estimation of our model by using maximum likelihood estimator was expressed in equation 1.

Maximize *The probability of the distance from the multi-centers* ＋*The probability of distance from the roads* ＋*The probability of class translation from non-urban to urban* (1)

Since the probability of class translation and the probabilities of the distance from the multi-centers and the distance from the roads are independent, we separated it into two parts with equation 2 and 3.

Maximize *The Probability of Class translation from non-urban to urban* (2)

Maximize *The probability of the distance from the multi-centers* ＋*The probability of the distance from the roads* (3)

Since non-urban refers to vegetation and water. Equation 2 is expressed with more details as the equation 4.

$$\text{Maximize } Pvegetation(t) \rightarrow urban(t+1) \text{ and } Pwater(t) \rightarrow urban(t+1),\ t=1,2,3,4 \tag{4}$$

Where $Pvegetation(t) \rightarrow urban(t+1)$ is the probability of class translation from vegetation at time t to urban at time t+1. $Pwater(t) \rightarrow urban(t+1)$ is the probability of class translation from water at time t to urban at time t+1. In this research, t=1 represents the year of 1978, t=2 represents the year of 1990, t=3 represents the year of 2000, t=4 represents the year of 2009. Equation 4 was converted into equation 5 as below.

$$\sum_{i=1,j=1}^{1000,1000} vegetation(i,j,t) \rightarrow urban(i,j,t+1) = N_{vegetation(t)\rightarrow urban(t+1)}$$

and

$$\sum_{i=1,j=1}^{1000,1000} water(i,j,t) \rightarrow urban(i,j,t+1) = N_{water(t)\rightarrow urban(t+1)},\quad t=1,2,3,4 \tag{5}$$

Where $vegetation(i,j,t)$ is vegetation at the pixel of (i, j) at time t and $urban(i,j,t+1)$ is urban at the pixel of (i, j) at time t+1. $water(i,j,t)$ is water at the pixel of (i, j) at time t and $urban(i,j,t+1)$ is urban at the pixel of (i, j) at time t+1. i and j are the locations of the images in x-axis and y-axis. $N_{vegetation(t)\rightarrow urban(t+1)}$ is the number of observed pixels that changed from vegetation at time t to urban at time t+1. $N_{vwater(t)\rightarrow urban(t+1)}$ is the number of observed pixels that changed from water at time t to urban at time t+1.

To express more details in equation 3, the equation 6 is written as below.

$$\text{Maximize}\prod_{i=1,j=1}^{1000,1000}\left[\beta_1^{1/2}\frac{1}{\sigma_{center}(t\rightarrow t+1,c)\sqrt{2\pi}}\exp\left(-\beta_1\frac{(disCenter(i,j,t+1)-\mu(t\rightarrow t+1,c)_{center})^2}{2\sigma(t\rightarrow t+1,c)^2_{center}}\right)\times\beta_2^{1/2}\frac{1}{\sigma_{road}\sqrt{2\pi}}\exp\left(-\beta_2\frac{(disRoad(i,j,t+1)-\mu_{road})^2}{2\sigma^2_{road}}\right)\right] \tag{6}$$

β_1 and β_2 control the variances of distributions ($\beta_1^{1/2}$ and $\beta_2^{1/2}$ are optional). They play roles as precision parameters. Since some parts of equation 6 are insignificant, and some parameters are constant, we omitted some insignificant parts in equation 6 and turn it into equation 7.

$$\text{Minimize}\sum_{i=1,j=1}^{1000,1000}\left[\beta_1\frac{(disCenter(i,j,t+1)-\mu(t\rightarrow t+1,c)_{center})^2}{\sigma(t\rightarrow t+1,c)^2_{center}}+\beta_2\frac{(disRoad(i,j,t+1)-\mu_{road})^2}{\sigma^2_{road}}\right] \tag{7}$$

Where $disCenter(i,j,t+1)$ is the Euclidean distance from the multi-centers of the urban areas at the pixels of (i, j) at time t+1. $disRoad(i,j,t+1)$ is the Euclidean distance from the roads at the pixels of (i, j) at time t+1. $\mu(t\rightarrow t+1,c)_{center}$ is the mean of the distances from the multi-centers of urban areas that were observed from time t to time t+1 at the center c.

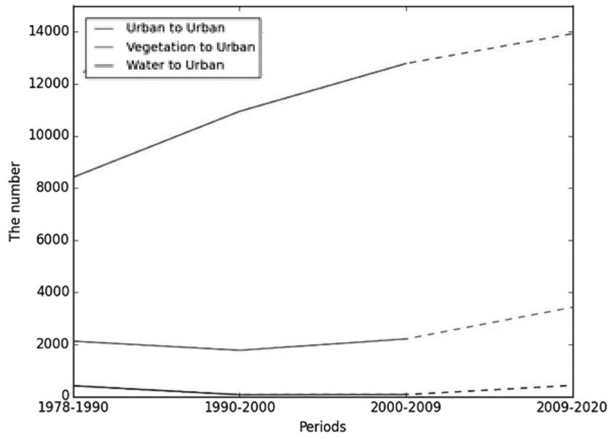

Fig. 10 The estimated class translation in the region of the center #1 in 2020 (The unit of pixel).

$\sigma(t\rightarrow t+1,c)^2_{center}$ is the variance of the distances from the multi-centers of the urban areas that were observed from time t to time t+1 at the center c. μ_{road} is the mean of the distances from the roads. σ^2_{road} is the variance of the distances from the roads. β_1 and β_2 are assumed as the weight coefficients or the precision parameters. In this research, since we found the urban grew up from near distance from the multi-centers of urban areas to the far distance, so we set the values of $\mu(t\rightarrow t+1,c)_{center}$ as zero since the urban grows up from the locations of multi-centers of urban areas. $\sigma(t\rightarrow t+1,c)^2_{center}$, μ_{road} and σ^2_{road} are assigned as the observed values in the step of 2.3 Monitoring urban expansion. β_1 and β_2 were required to be assigned. By varying values of the coefficients of β_1 and β_2 with three cases (large β_1 ($\beta_1=0.7$ and $\beta_2=0.3$), small β_1 ($\beta_1=0.3$ and $\beta_2=0.7$), equal β_1 to β_2 ($\beta_1=0.5$ and $\beta_2=0.5$)), we found that $\beta_1=0.5$ and $\beta_2=0.5$ that provided the highest accuracy (see table 5). In implementing the process, the equation 5 and 7 were simultaneously maximized to calculate urban expansion.

The classification result in 1978 was set as the initial land cover image. We used the initial land cover image with the observed parameters as input for our model to estimate the land cover images in 1990. Next, we used the estimated land cover in 1990 with the observed parameters as input for our model to estimate the land cover image in 2000. We repeated the similar step to estimate the land cover image in 2009.

2.5 The prediction of urban expansion

Since all the parameters in the future could not be observed such as the class translation and the mean and variance of the distances from the multi-centers of urban areas. They are required to be estimated. We used the previous information that can be observed with the polynomial regression[12] to calculate all the parameters in the future. The polynomial regression is a form of linear regression which is commonly used for trend analysis. In this research, we estimated the urban areas in 2020 as the

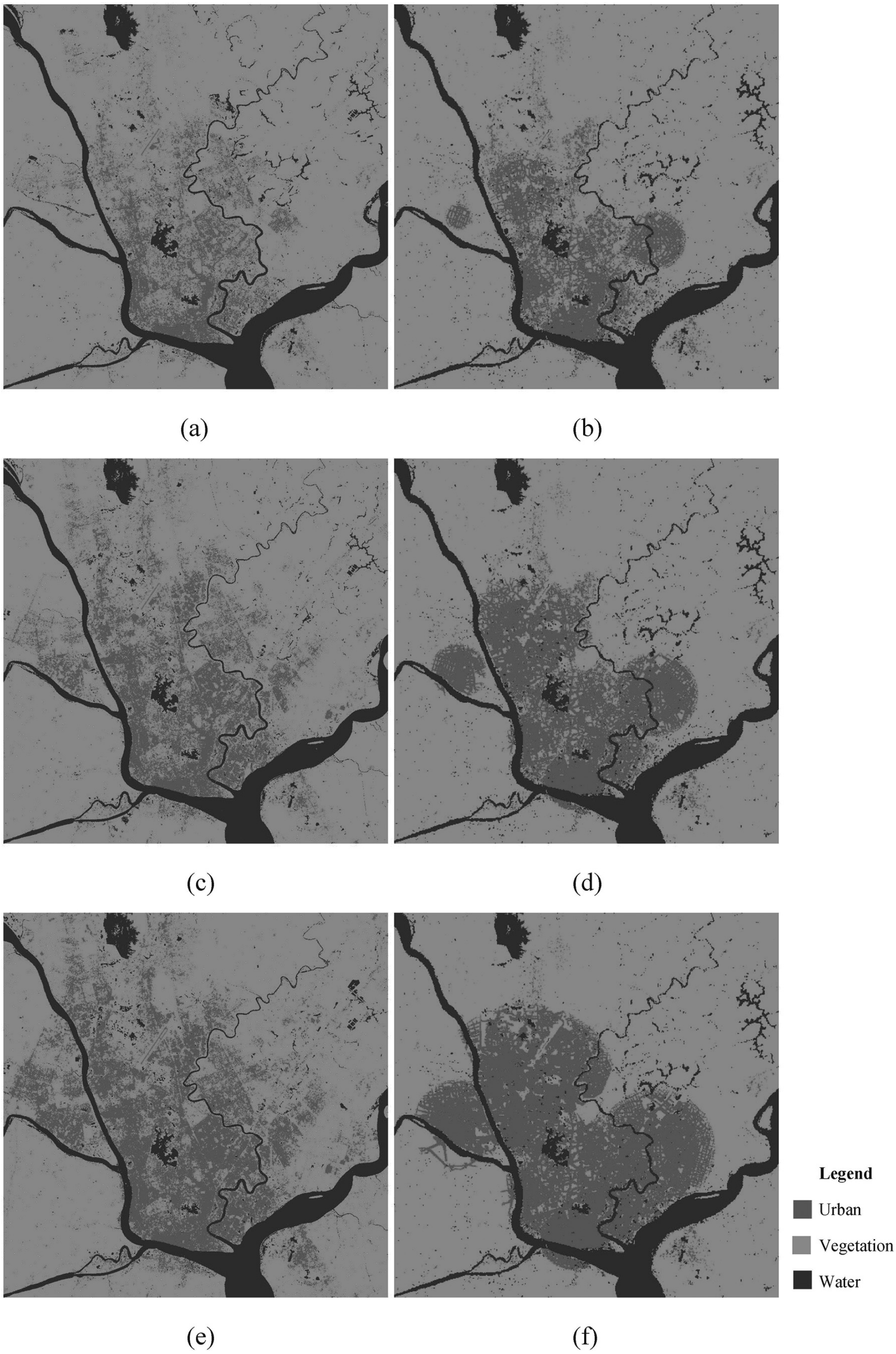

Fig. 11 (a) the referenced land cover image in 1990, (b) the estimated land cover image in 1990, (c) the referenced land cover image in 2000, (d) the estimated land cover image in 2000, (e) the referenced land cover image in 2009, and (f) the estimated land cover image in 2009.

future time. The parameters in 2020 were estimated by using the polynomial regression with the second degree. The example of estimated parameter of the class translation matrix in the region of the center #1 is shown in figure 10.

After that, we used the estimated land cover in 2009 with estimated parameters as input for our model to predict the land cover image in 2020.

3. Results and discussions

3.1 The estimation of urban expansion

The classification results in the section of 2.2 preparing data for urban expansion were defined as the referenced land cover images. We compared the estimated land cover images by using our model (figure 11 (b, d, f)) with the referenced land cover images (figure 11 (a, c, e)). For the accuracy, two classes with urban and non-urban (vegetation and water) were used to calculate the accurate result. The accuracies of the estimated versus the referenced land cover images in 1990, 2000, and 2009 are expressed in table 4.

In additional, the accuracies of our estimation by varying the weight coefficients of β_1 and $\beta_2$with three experiments is shown in table 5.

3.2 The prediction of urban expansion

The Landsat image on November 25, 2015 (figure 12 (a)) was selected and classified to be a land cover image as an unseen land cover image (figure 12 (b)). We compared the predicted land cover image in 2020 (figure 10 (c)) with the unseen land cover image in 2015. The accuracy is 81.24 % with the true positive rate of 70.86 % and the true negative rate of 85.64 %.

Furthermore, another index of Nest/Nref was calculated for the validation of estimating the non-urbanàurban. Nest and Nest are the numbers of pixels that changed from non-urban to urban by the estimation and by the reference classification, respectively. The Nest/Nref indexes of estimation and prediction of urban expansion are shown in table 6.

Table 4 The accuracies of the estimated versus the referenced urban areas in 1990, 2000, and 2009.

Year	Accuracy (%)	True positive rate (%)	True negative rate (%)
1990	93.52	65.01	96.52
2000	88.58	62.13	93.38
2009	84.03	64.38	89.82
Average	88.71	63.84	93.24

3.3 Discussions

According to figure 11 and table 4, our model of urban expansion estimated the urban growth in the years of 1990, 2000, and 2009 with the averaged accuracy of 88.71 % with averaged true positive rate of 63.84 % and averaged true negative rate of 93.24 %. As well as, our model predicted the urban expansion in the future (in the year of 2020) with the accuracy of 81.32 % with the true positive rate of 71.02 % and the true negative rate of 85.68 %.

According to table 5, we found that $\beta_1 = 0.5$ and $\beta_2 = 0.5$ gave the highest accuracy. However, by varying β_2 and β_2 with three experiments, it made slightly different results. Also, we investigated that the model is significantly controlled by the variances since the variances between the distances from the multi-centers of urban areas and the distances from roads are very different (σ^2_{center} is very large and σ^2_{road} is very small). As a result, the distances from the roads are more impact to urban expanding than the distances from the multi-centers center of the urban area. On the other hand, it can be assumed that in Yangon, firstly, people consider creating houses or buildings near roads and secondly, they create the houses or buildings near the multi-centers of urban areas.

Since our proposed method uses the statistical parameters to support in the estimation of urban expansion, the expansion areas could be well estimated following the defined factors. Whereas, the previous method without considering on the statistical parameters [6] is not expected to offer such result because there are no dynamic statistical parameters to support controlling the levels of impacts of the defined factors in the estimation of urban expansion.

In our model, we only used the road data for transportation. In Yangon, there are railways for transportation. Possibly, the urban expansion should rely on the railways. Also, we only used the land covers for environmental factor. In Yangon, the terrains are mixed between small mountain and flat areas. The urban expansion may be affected by the elevations. Therefore, our results were incorrect for some urban expansion areas affected by

Table 5 The averaged accuracies of the estimated versus the referenced urban areas in 1990, 2000, and 2009 by varying weight coefficients.

Weight coefficients	Averaged Accuracy (%)	Averaged true positive rate (%)	Averaged true negative rate (%)
$\beta_1 = 0.3,\ \beta_2 = 0.7$	88.53	63.33	93.13
$\beta_1 = 0.5,\ \beta_2 = 0.5$	88.71	63.84	93.24
$\beta_1 = 0.7,\ \beta_2 = 0.3$	88.66	63.81	93.20

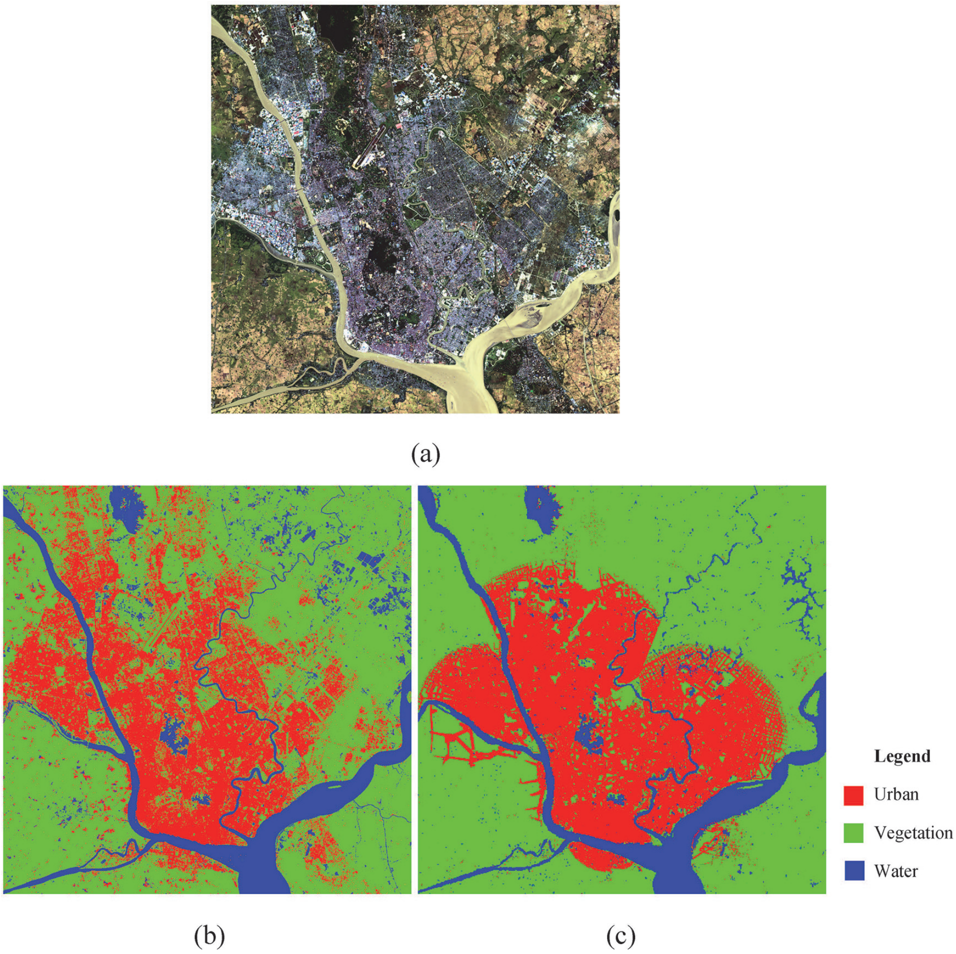

Fig. 12 (a) the Landsat image in 2015, (b) the referenced land cover image in 2015, and (c) the predicted land cover image in 2020.

Table 6 The index of Nest/Nref.

Urban expansion (non-urban → urban)	Nest/Nref
1990	0.193
2000	0.238
2009	0.179
2020	0.175
Overall without specific period	0.648

those factors. To improve the results, the other factors such as railway, elevation should be included in the model. Furthermore, since our model relies on the distance from the multi-centers of the urban areas, the estimated urban areas grew up from the closest distance from the multi-centers of the urban area. However, In particular, some urban areas grew up far from the multi-centers of the urban areas because of economic reason since the land price is cheaper. As a result, our method cannot estimate the urban areas that grow up far from the multi-centers of the urban areas and it made the incorrect results.

In addition, for setting the parameters, since the parameters of β_1 and β_2 are needed to set up by manual method, the optimization searching method with fewer computations can be used to find the finest parameters for the model to archive the higher accuracy. Furthermore, in the model, the probability of the distance from the roads should be defined as the Gamma distribution. Thus, the integrating multiple distributions (the Gaussian and Gamma distributions) can be applied to the urban expansion model for the higher reliability.

For the prediction of the urban expansion, the future parameters cannot be observed and the roads can be created also the multi-centers can be changed. Hence, the predicted result seemed not reliable. In order to provide more reliability in the predicted result, the main plan relating to urban expansion by the government or authorizing office is necessary to be used for calculating those parameters.

For the index of Nest/Nref, our estimated results have low values. Since the estimated urban expansions have the low distributions of urban expansions since our model only focuses on three factors; especially the multi-centers of urban areas, while the referred urban expansions have the high distributions causing from not only the three factors but also other factors such as railways, elevations, economic states etc. However, when calculating the overall index of Nest/Nref without a specific period. Our method has the high index of 0.65 since the trending of urban expansion relies on the multi-centers of the urban areas.

To understand deeply the mechanism of the urban expansion, the significant structures such as commercial buildings, government offices, plants, transportations, and bridges can be related to our model.

4. Conclusions

This research introduced a methodology to model urban expansion using Landsat time-series and stereo GeoEye images in Yangon, Myanmar. Multispectral Landsat images from 1978 to 2009 were used to provide land cover change. Stereo GeoEye images were employed to extract the heights of buildings that can be used to detect the multi-centers of urban areas. The model of urban expansion was defined to refer three factors of (1) the distances from the multi-centers of the urban areas, (2) the distances from the roads and (3) the class translation. Based on the dynamic statistical model, the estimation of urban expansion was formulated by using the maximum likelihood estimator. The prediction of urban expansion was calculated by using polynomial regression. In the experimental results, our method estimated urban areas from 1990, 2000, 2009 with the averaged accuracy of 88.71 % and predicted urban areas in 2020 with the accuracy of 81.32 %. The urban expansion results indicated that our proposed method based on the dynamic statistical model with the defined factors estimated urban expansion with efficiency since the dynamic statistical parameters cloud be used to support controlling the degrees of impacts of the defined factors in the estimation of urban expansion.

In addition, in order to improve the accuracy, the other factors such as railways and elevations should be included in our model. Since some parameters are required to specify, the optimization method could be employed. To provide more reliability in the prediction of urban expansion, the main plan relating to urban expansion by authorizing office is necessary to be used for calculating the future parameters in the model. To deeply understand the practical mechanism of urban expansion, the significant structure such as commercial buildings, government offices, and transportations can be related to our model.

Acknowledgment

This research was supported by Japan Science and Technology Agency (JST)/ Japan International Cooperation Agency (JICA), Science and Technology Research Partnership for Sustainable Development Program (SATREPS).

References

1) I. Morley: Rangoon, Cities, 31, pp. 601–614, 2013.

2) H. Bagan and Y. Yamagata: Landsat analysis of urban growth: How Tokyo became the world's largest megacity during the last 40 years, Remote Sensing of Environment, 127, pp. 210–222, 2012.

3) K. C. Clarke and L. J. Gaydos: Loose-coupling a cellular automaton model and GIS: long-term urban growth prediction for San Francisco and Washington/Baltimore, International Journal of Geographical Information Science, 12 (7), pp. 699–714, 1998.

4) I. S. Lowry: A model of metropolis Santa Monica, CA (Rand Corporation), 1964.

5) F. H. Sklar and R. Costanza: The development of dynamic spatial models for landscape ecology, A review and prognosis, pp. 239–288, 1991.

6) M. Batty: Cellular automata and urban form (A primer), Journal of the American Planning Association, 63 (3), pp. 264–274, 1997.

7) I. Benenson: Multiagent simulations of residential dynamics in the city, Computers Environment and Urban Systems, 22 (1), pp. 25–42, 1998.

8) A. G. Wilson: Catastrophe Theory and Bifurcation Application to Urban and Regional Systems, Croom Helm, London, pp. 55–79, 1981.

9) X. Zhang and Y. Wang: Spatial Dynamic Modeling for Urban Development, Photogrammetric Engineering & Remote Sensing, 67 (9), pp. 1049–1057, 2001.

10) R. D. Maesschalck, D. Jouan-Rimbaud and D. L. Massart: The Mahalanobis distance, Chemometrics and Intelligent Laboratory Systems, 50, pp. 1–18, 2000.

11) S. H. Cho, Z. Chen, S. T. Yen and D. B. Eastwood: Estimating Effects of an Urban Growth Boundary on Land Development, Journal of Agricultural and Applied Economics, 38 (2), pp. 287–298, 2006.

12) S. Greenland: Dose-Response and Trend Analysis in Epidemiology: Alternatives to Categorical Analysis, Epidemiology, Lippincott Williams & Wilkins, 6 (4), pp. 356–365, 1995.

〔**Author's biography**〕

● **Mr. Tanakorn Sritarapipat** has been a Ph.D. student with MEXT scholarship in Civil Engineering at The University of Tokyo, Japan since 2014. He graduated both Bachelor and Master degrees in Electrical Engineering from Kasetsart University, Thailand in 2008 and 2011, respectively. He had worked as a researcher at Geo-Informatics and Space Technology Development Agency (GISTDA), Thailand from 2011 to 2014. His research field has been related to Remote sensing, Geographic Information Systems and Digital Image Processing with the various applications such as modeling urban expansion, disaster management, and agriculture tools.

E-mail : tanakorn@iis.u-tokyo.ac.jp

● **Dr. Wataru Takeuchi** is currently an Associate Professor at Institute of Industrial Science (IIS), The University of Tokyo, Japan. He obtained Bachelor degree in 1999, Master degree in 2001, and a Ph.D. degree in 2004 at Department of Civil Engineering, Faculty of Engineering, The University of Tokyo, Japan. He has worked at IIS since 2004 as a Postdoctoral fellow. Dr. Wataru Takeuchi was a Visiting Assistant Professor at Asian Institute of Technology (AIT), Thailand from 2007 to 2009. He was also Director of Japan Society for Promotion of Science (JSPS), Bangkok office, Thailand from 2010 to 2012. He has been a regular member of Japan Society of Photogrammetry and Remote Sensing, Remote Sensing Society of Japan, American Geophysical Union, and American Society of Photogrammetry and Remote Sensing. His current research interests consist of Remote Sensing.

E-mail : wataru@iis.u-tokyo.ac.jp